The Astronomical Journal, 130:2598–2612, 2005 December

THE ARECIBO LEGACY FAST ALFA SURVEY. I. SCIENCE GOALS, SURVEY DESIGN, AND STRATEGY

Riccardo Giovanelli,[1] Martha P. Haynes,[1] Brian R. Kent,[1] Philip Perillat,[2] Amelie Saintonge,[1] Noah Brosch,[3] Barbara Catinella,[2] G. Lyle Hoffman,[4] Sabrina Stierwalt,[1] Kristine Spekkens,[1] Mikael S. Lerner,[2] Karen L. Masters,[1] Emmanuel Momjian,[2] Jessica L. Rosenberg,[5] Christopher M. Springob,[1] Alessandro Boselli,[6] Vassilis Charmandaris,[7] Jeremy K. Darling,[8] Jonathan Davies,[9] Diego Garcia Lambas,[10] Giuseppe Gavazzi,[11] Carlo Giovanardi,[12] Eduardo Hardy,[13] Leslie K. Hunt,[14] Angela Iovino,[15] Igor D. Karachentsev,[16] Valentina E. Karachentseva,[17] Rebecca A. Koopmann,[18] Christian Marinoni,[15] Robert Minchin,[9] Erik Muller,[19] Mary Putman,[20] Carmen Pantoja,[21] John J. Salzer,[22] Marco Scodeggio,[23] Evan Skillman,[24] Jose M. Solanes,[25] Carlos Valotto,[10] Wim van Driel,[26] and Liese van Zee[27]

Received 2005 May 17; accepted 2005 August 5

ABSTRACT

The recently initiated Arecibo Legacy Fast ALFA (ALFALFA) survey aims to map $\sim$7000 deg^2 of the high Galactic latitude sky visible from Arecibo, providing a H I line spectral database covering the redshift range between -1600 and 18,000 km s^{-1} with $\sim$5 km s^{-1} resolution. Exploiting Arecibo's large collecting area and small beam size, ALFALFA is specifically designed to probe the faint end of the H I mass function in the local universe and will provide a census of H I in the surveyed sky area to faint flux limits, making it especially useful in synergy with wide-area surveys conducted at other wavelengths. ALFALFA will also provide the basis for studies of the dynamics of galaxies within the Local Supercluster and nearby superclusters, allow measurement of the H I diameter function, and enable a first wide-area blind search for local H I tidal features, H I absorbers at $z < 0.06$, and OH megamasers in the redshift range $0.16 < z < 0.25$. Although completion of the survey will require some 5 years, public access to the ALFALFA data and data products will be provided in a timely manner, thus allowing its application for studies beyond those targeted by the ALFALFA collaboration. ALFALFA adopts a two-pass, minimum intrusion, drift scan observing technique that samples the same region of sky at two separate epochs to aid in the discrimination of cosmic signals from noise and terrestrial interference. Survey simulations, which take into account large-scale structure in the mass distribution and incorporate experience with the ALFA system gained from tests conducted during its commissioning phase, suggest that ALFALFA will detect on the order of 20,000 extragalactic H I line sources out to $z \sim 0.06$, including several hundred with H I masses $M_{\rm H\,I} < 10^{7.5}\,M_\odot$.

Key words: galaxies: distances and redshifts — galaxies: halos — galaxies: luminosity function, mass function — galaxies: photometry — galaxies: spiral — radio lines: galaxies — surveys

[1] Center for Radiophysics and Space Research and National Astronomy and Ionosphere Center, Cornell University, Ithaca, NY 14853; riccardo@astro.cornell.edu, haynes@astro.cornell.edu, bkent@astro.cornell.edu, amelie@astro.cornell.edu, sabrina@astro.cornell.edu, spekkens@astro.cornell.edu, masters@astro.cornell.edu, springob@astro.cornell.edu.

[2] Arecibo Observatory, National Astronomy and Ionosphere Center, Arecibo, PR 00612; bcatinel@naic.edu, lerner@naic.edu, phil@naic.edu, emomjian@naic.edu.

[3] The Wise Observatory and The School of Physics and Astronomy, Raymond and Beverly Sackler Faculty of Exact Sciences, Tel Aviv University, Tel Aviv 69978, Israel; noah@wise.tau.ac.il.

[4] Hugel Science Center, Lafayette College, Easton, PA 18042; hoffmang@lafayette.edu.

[5] Harvard-Smithsonian Center for Astrophysics, 60 Garden Street, MS 65, Cambridge, MA 02138-1516; jlrosenberg@cfa.harvard.edu.

[6] Laboratoire d'Astrophysique, Traverse du Siphon, BP8, 13376 Marseille, France; alessandro.boselli@oamp.fr.

[7] Department of Physics, University of Crete, 71003 Heraklion, Greece; vassilis@physics.uoc.gr.

[8] Carnegie Observatories, 813 Santa Barbara Street, Pasadena, CA 91101; darling@ociw.edu.

[9] Department of Physics and Astronomy, University of Wales, Cardiff CF24 3YB, UK; jonathan.davies@astro.cf.ac.uk, robert.minchin@astro.cf.ac.uk.

[10] Observatorio Astronómico, Universidad Nacional de Córdoba, Cordoba 5000, Argentina; dgl@oac.uncor.edu, val@oac.uncor.edu.

[11] Dipartimento di Fisica, Universitá di Milano-Bicocca, Milan 20126, Italy; giuseppe.gavazzi@mib.infn.it.

[12] INAF—Osservatorio Astrofisico d'Arcetri, Largo Enrico Fermi 5, 50125 Florence, Italy; giova@arcetri.astro.it.

[13] National Radio Astronomy Observatory, Apoquindo 3650, Piso 18, Las Condes, Santiago, Chile; ehardy@nrao.edu.

[14] INAF—Istituto di Radioastronomia, Sezione Firenze, Largo Enrico Fermi 5, 50125 Florence, Italy; hunt@arcetri.astro.it.

[15] INAF—Osservatorio Astronomico di Brera, Via Brera 28, 20121 Milan, Italy; iovino@brera.mi.astro.it, marinoni@brera.mi.astro.it.

[16] Special Astrophysical Observatory, Russian Academy of Sciences, Niszhnij Arkhyz 369167, Zelencukskaya, Karachai-Cherkessia, Russia; ikar@sao.ru.

[17] Department of Astronomy and Space Science, Kiev University, Kiev 252017, Ukraine; vkarach@observ.univ.kiev.ua.

[18] Department of Physics and Astronomy, Union College, Schenectady, NY 12308; koopmanr@union.edu.

[19] Australia Telescope National Facility, CSIRO, P.O. Box 76, Epping, NSW 1710, Australia; erik.muller@atnf.csiro.au.

[20] Astronomy Department, University of Michigan, Ann Arbor, MI 48109; mputman@umich.edu.

[21] Department of Physics, University of Puerto Rico, P.O. Box 364984, San Juan, PR 00936; cpantoja@naic.edu.

[22] Astronomy Department, Wesleyan University, Middletown, CT 06457; slaz@astro.wesleyan.edu.

[23] Dipartimento di Fisica, Universitá di Milano, Via Celoria 16, 20133 Milan, Italy; marcos@mi.iasf.cnr.it.

[24] Astronomy Department, University of Minnesota, 116 Church Street SE, Minneapolis, MN 55455; skillman@astro.umn.edu.

[25] Department d'Astronomia i Meteorologia, Universidad de Barcelona, Avenida Diagonal 647, 08028 Barcelona, Spain; and Centre Especial de Recerca en Astrofísica, Física de Partícules i Cosmologia, associated with the Instituto de Ciencias del Espacio, Consejo Superior de Investigaciones Científicas; jm.solanes@ub.edu.

[26] Observatoire de Meudon, 5 Place Jules Janssen, 92195 Meudon, France; wim.vandriel@obspm.fr.

[27] Astronomy Department, Indiana University, Bloomington, IN 47405; vanzee@astro.indiana.edu.

1. INTRODUCTION

The first 21 cm line detection of an extragalactic source (the Magellanic Clouds) was achieved by Kerr & Hindman (1953) with a 36 foot (11 m) transit telescope just over half a century ago. The construction of large, single-dish radio telescopes produced seminal discoveries in the 1960s, as illustrated in the fundamental paper of that period (Roberts 1975). A decade later, the completion of the Very Large Array (VLA) and the Westerbork Synthesis Radio Telescope, the resurfacing of the Arecibo dish, and rapid progress in detector and spectrometer technology made it possible for H I spectroscopy to achieve order-of-magnitude improvements in terms of sensitivity and resolution. New scientific problems became accessible, and extragalactic H I line research underwent a phase of rapid growth. The study of rotation curves led to the discovery of dark matter in spiral galaxies, the potential of the luminosity–line width relation as a cosmological tool became apparent, and the impact of tidal interactions and the intracluster medium on galaxy evolution was illustrated in great detail through measures of the H I emission. The 21 cm line was found to be an expedient tool to determine accurate galaxy redshifts, playing an important role in confirming the filamentary nature of the large-scale structure of the universe. The application of the luminosity–line width relation led to accurate estimates of cosmological parameters and the characterization of the peculiar velocity field in the local universe. Highly sensitive measurements in the peripheries of disk galaxies revealed edges in their visible components, and a number of optically inert objects were discovered.

Until a few years ago, however, comprehensive wide-angle surveys of the extragalactic H I sky were unavailable. At the close of the last decade, the advent of multifeed front-end systems at the *L* band finally made possible the efficient coverage of large sections of the extragalactic sky. The first such system to be used for that purpose was installed on the 64 m Parkes telescope in Australia and has produced the excellent results of the H I Parkes All-Sky Survey (HIPASS; Barnes et al. 2001; Meyer et al. 2004). A second four-feed system on the 76 m Lovell Telescope at Jodrell Bank produced the H I Jodrell All-Sky Survey (HIJASS; Lang et al. 2003). The 1990s upgrade of the Arecibo telescope, which replaced its line feeds with a Gregorian subreflector system, made it possible for that telescope to host feed arrays, as proposed by Kildal et al. (1993). Eventually built and installed at Arecibo in 2004, this seven-beam radio "camera," named ALFA (Arecibo L-band Feed Array), is now operational, enabling large-scale mapping projects with the great sensitivity of the 305 m telescope. A diverse set of mapping projects are now under way, ranging from extragalactic H I line to Galactic line and continuum to pulsar searches. Here we introduce one of these newly initiated surveys, specifically designed to map approximately one-fifth of the sky in the H I line out to a distance of 250 Mpc. The survey, currently under way at Arecibo, is referred to as ALFALFA (Arecibo Legacy Fast ALFA) survey.

As illustrated in Figure 1, ALFALFA aims to cover 7074 deg^2 of the high Galactic latitude sky between 0° and 36° in declination, requiring a total of 4130 hr of telescope time. Exploiting the large collecting area of the Arecibo antenna and its relatively small beam size (∼3.′5), ALFALFA will be nearly 8 times more sensitive than HIPASS with ∼4 times better angular resolution. Furthermore, its spectral back end provides 3 times better spectral resolution (5.3 km s^{-1} at $z = 0$) over 1.4 times more bandwidth. These advantages, in combination with a simple observing technique designed to yield excellent baseline characteristics, flux calibration, and H I signal verification, offer new opportunities to explore the extragalactic H I sky. Data taking for ALFALFA was initiated in 2005 February, and, in the practical context of time allocation at a widely used, multidisciplinary national facility like Arecibo, completion of the full survey is projected to require 5–6 yr.

As discussed in § 4.2, simulations predict that ALFALFA will detect some 20,000 extragalactic H I line sources, from very nearby low-mass dwarfs to massive spirals at $z \sim 0.06$. The survey is specifically designed to robustly determine the faint end of the H I mass function (HIMF) in the local universe at masses $M_{\rm H\,I} < 10^8\ M_\odot$ and will at the same time provide a census of H I in the surveyed sky area, making it especially useful in synergy with other wide-area surveys such as the Sloan Digital Sky Survey (SDSS), the Two Micron All Sky Survey (2MASS), the *Galaxy Evolution Explorer* (*GALEX*), *ASTRO-F*, etc. In conjunction with optical studies of comparable volumes, ALFALFA will help determine the true census of low-mass satellites and the widely distributed dwarf galaxy population in the Local Group and surrounding groups. Its data set will also provide the basis for studies of the dynamics of galaxies within the Local Supercluster and nearby superclusters, allow measurement of the H I diameter function, and enable a first wide-area blind search for local H I tidal features, H I absorbers at $z < 0.06$, and OH megamasers (OHMs) in the redshift range $0.16 < z < 0.25$. Survey details and status can be found by visiting the survey Web site.[28]

Survey efforts of this scale and scope require careful optimization of their operational strategy toward achieving the science objectives within the constraints imposed by practical observing conditions and requirements. In this paper, we introduce the science objectives of ALFALFA, the principal constraints that set its strategy, and the results of survey simulations that allow prediction of its eventual results. In a companion paper (Giovanelli et al. 2005, hereafter Paper II), we present results obtained during a precursor observing run, designed to allow us to test and optimize the ALFALFA strategy during the ALFA commissioning phase in fall 2004.

We summarize, in § 2, the main scientific motivations of the survey. Technical details of the hardware are given in § 3, while criteria leading to the design of the survey, in the form of scaling laws and survey simulations, are described in § 4. Observing modes, sky tiling, and data processing plans are presented in § 5, while § 6 summarizes sensitivity numbers at various stages of the survey. We elaborate on the treatment of candidate detections and follow-up observations in § 7 and summarize in § 8. Throughout the paper, we assume $H_0 = 70$ km s^{-1} Mpc^{-1}.

2. OVERVIEW OF ALFALFA SCIENCE GOALS

Following on the results of a number of important and successful previous blind H I surveys, extragalactic H I surveys with ALFA will exploit Arecibo's huge collecting area to explore larger volumes of the universe with greater sensitivity and higher angular and spectral resolution if they are to break new science ground. With Arecibo's tremendous sensitivity and beam size advantages, ALFALFA is designed for wide areal coverage, thereby increasing the volume sampled locally, yielding a deep, precise census of H I in the local universe to the lowest H I masses.

ALFALFA aims to survey 7074 deg^2 of sky at high Galactic latitudes that lie within the declination limits of the Arecibo telescope, $-2° < \text{decl.} < +38°$, as illustrated in Figure 1. Based

[28] See http://egg.astro.cornell.edu/alfalfa.

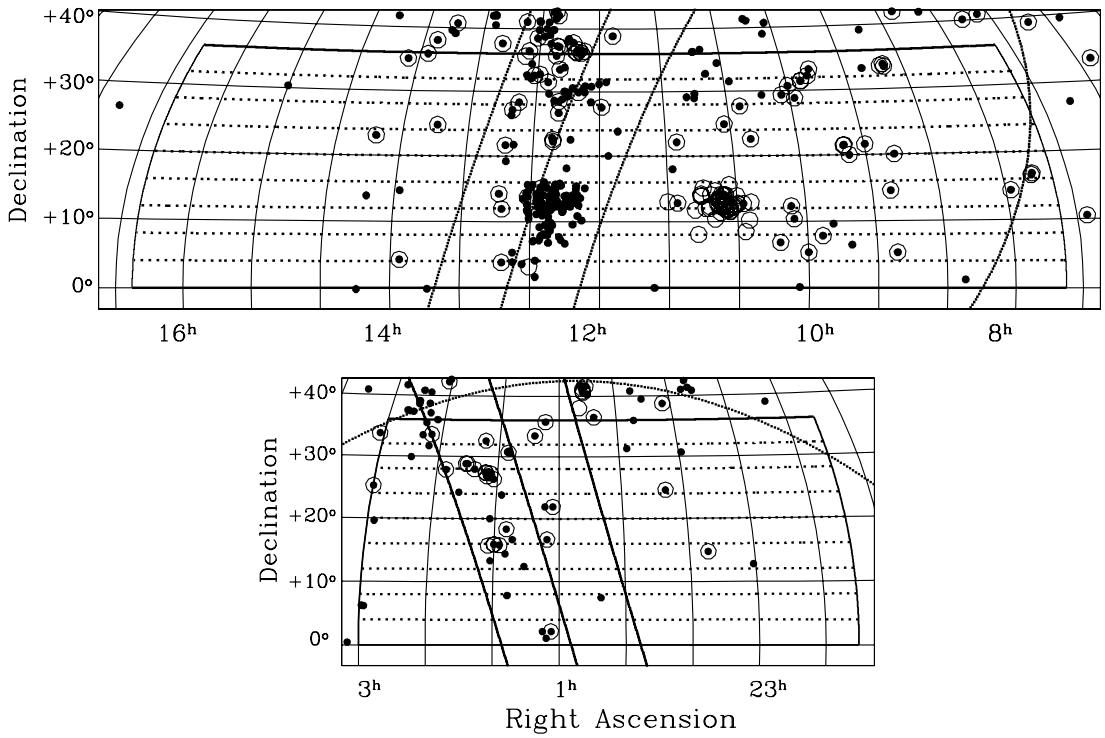

FIG. 1.—Proposed sky coverage of the ALFALFA survey in the Virgo (*top*) and anti-Virgo (*bottom*) directions. In each panel, the thick lines at constant right ascension or declination outline the proposed survey area. Dashed lines at constant declination mark the designated ALFALFA tile strip boundaries. The thick dotted curves at the right of the top panel and the top of the bottom panel indicate $b = +20^\circ$ (*top*) and -20° (*bottom*), while the set of three thick solid lines crossing each panel vertically traces SGL $= -10^\circ$, 0°, and $+10^\circ$. Filled circles represent galaxies with observed heliocentric recessional velocities $cz < 700$ km s^{-1}, while open circles denote objects believed to lie within 10 Mpc (Karachentsev et al. 2004), based largely on primary distances.

on simulations described in § 4.2 and now verified by the results of the ALFALFA precursor observations presented in Paper II, ALFALFA is expected to yield on the order of 20,000 H I line detections, sampling a wide range of sources from local, very low H I mass dwarfs to gas-rich massive galaxies seen to $z \sim 0.06$ ($\sim$250 Mpc). H I spectra provide redshifts, H I masses, and rotational widths for normal galaxies, trace the history of tidal events with high kinematical accuracy, and provide quantitative measures of the potential for future star formation via comparative H I contents. As a blind H I survey, ALFALFA will not be biased toward the high surface brightness galaxies typically found in optical galaxy catalogs and, moreover, in contrast to HIPASS and HIJASS, will have adequate angular and spectral resolution to be used on its own, generally without the need for follow-up observations to determine identifications, positions, and, in many cases, H I sizes. The wide areal coverage of ALFALFA overlaps with several other major surveys, most notably the SDSS, 2MASS, and the NRAO VLA Sky Survey. The catalog products of ALFALFA will be invaluable for multiwavelength data mining for a wide spectrum of purposes, and a key element of our overall collaborative program is to provide broad application, legacy data products that will maximize the science fallout of the ALFALFA survey.

A primary objective of ALFALFA is the robust determination of the faint end of the HIMF. The HIMF is the cosmic number density per bin of H I mass of detectable H I line signals in a survey sensitive to the global neutral hydrogen within a system. The most recent estimates of the HIMF based on significant numbers of galaxies have been presented by Zwaan et al. (1997, hereafter Z97), Rosenberg & Schneider (2002, hereafter RS02), Zwaan et al. (2004, hereafter Z04), Zwaan et al. (2005, hereafter Z05), and Springob et al. (2005a). The Z04 and Z05 HIMFs are based on the HIPASS survey, while the RS02 and Z97 HIMFs are based on surveys conducted at Arecibo during the period of its recent upgrade. The faint-end slope of those determinations of the HIMF vary between -1.20 and -1.53, yielding extrapolations below $M_{\rm H\,I} = 10^7\ M_\odot$ that disagree by an order of magnitude near $10^6\ M_\odot$, the RS02 HIMF having the steeper slope. All of the previous H I blind surveys sample a lower mass limit just below $M_{\rm H\,I} = 10^8\ M_\odot$. No extragalactic H I sources were detected by RS02 or Z97 with $M_{\rm H\,I} < 10^7\ M_\odot$, while three are claimed by Z04, and only a small number of detections have $M_{\rm H\,I} < 10^8\ M_\odot$. We note that the distances of those detections are highly uncertain, for they are very nearby and the impact of peculiar velocity on the observed redshift is quite large, as pointed out by Masters et al. (2004). Thus, current inferences on the behavior of the HIMF at low mass levels are quite unreliable, as they are based on very few objects of highly uncertain distance.

With the aim of exploring the HIMF at masses $M_{\rm H\,I} < 10^8\ M_\odot$, ALFALFA will cover a very large solid angle in order to survey an adequate volume at $D < 20$ Mpc, a distance within which the low H I mass systems are detectable. As shown by the simulations described in § 4.2, ALFALFA will detect several hundred objects with $M_{\rm H\,I} < 10^{7.5}\ M_\odot$. In addition, its extensive catalog of more massive objects will allow comparison of the high-mass end, $M_{\rm H\,I} > 10^9\ M_\odot$, in the diverse range of environments found in the volume out to 250 Mpc. The Arecibo sky to be surveyed by ALFALFA, as shown in Figure 1, includes the rich central regions of the Local Supercluster and the nearby low-density anti-Virgo region, as well as a number of more distant large-scale features, most notably the main ridge of the Pisces-Perseus supercluster and the Great Wall connecting the A1367-Coma and Hercules superclusters.

At the Virgo distance, ALFALFA should detect galaxies with H I masses as low as $M_{\odot} \sim 10^7$. ALFALFA will cover more than 1000 deg^2 around Virgo, yielding a database of unprecedented breadth for combination with the SDSS, *GALEX*, and other surveys to construct a complete census of baryon-bearing objects in the cluster and its full infall region. The combination of H I content, H I distribution, and the derived kinematical information with other multiwavelength studies will enable detailed modeling of the relative efficiency of gas-stripping mechanisms, such as tides, ram pressure, or galaxy harassment, as the origin of gas deficiency in Virgo. ALFALFA's H I maps will trace intriguing H I features such as the Virgo "dark cloud" (Davies et al. 2004; Minchin et al. 2005), the H I "plume" around NGC 4388 (Oosterloo & van Gorkom 2005), and the huge envelope surrounding NGC 4532 and DDO 137 (Hoffman et al. 1992). In more quiescent regions than Virgo, extensive tidal features such as the Leo triplet (Haynes et al. 1979) and enigmatic systems such as the 200 kpc Leo ring (Schneider et al. 1983) may be found. ALFALFA will enable the first truly blind survey for H I tidal remnants with both sufficient angular resolution and wide areal coverage to verify their nature.

While H I appendages uncover past disruptive events in galaxy evolution, extended gas disks around galaxies represent a reservoir for future star formation activity. In contrast to HIPASS and HIJASS, which were limited by much poorer angular resolution (15.′5 and 12′, respectively), the 3.′5 beam of ALFA will resolve the H I disks of ~500 gas-rich galaxies, allowing a quantitative measure of their H I sizes (Hewitt et al. 1983) and the derivation of the H I diameter function. In combination with optical photometry, ALFALFA will determine the fraction of galaxies with extended gas disks and enable studies of their host galaxies, environments, and morphologies and the role of gas in their evolution. More extremely extended gas disks, such as those found in DDO 154 (Krumm & Burstein 1984), UGC 5288 (van Zee 2005), and NGC 3741 (Begum et al. 2005), may yet lurk unidentified. Because of its wide sky coverage, ALFALFA will trace important high-velocity cloud (HVC) structures in and around the Milky Way, such as the northern portions of the Magellanic Stream and Complex C, at several times better spatial and spectral resolution than HIPASS, particularly important advantages in the case of narrow line width HVC cores (Giovanelli & Brown 1973). Because of its high flux sensitivity, ALFALFA will be 8 times more sensitive than HIPASS to unresolved small clouds, or ultracompact HVCs. While Arecibo cannot reach as far north as M31, ALFALFA will cover part of the region containing the clouds in its periphery identified by Thilker et al. (2004) and their possible extension toward the region around M33 (Westmeier et al. 2005).

In addition to the study of H I in emission, ALFALFA will provide a data set well suited for a blind survey of H I absorption out to $z \sim 0.06$. The background continuum source counts in the ALFALFA survey region at 1.4 GHz yield more than 2000 sources brighter than 0.4 Jy and more than 10,000 brighter than 0.1 Jy. The major practical difficulty with H I line absorption studies is spectral baseline determination in the presence of standing waves. The large number of continuum sources present in the ALFALFA data set and the adopted drift technique (§ 5.1) will aid in the assessment of whether a given spectral feature is real absorption.

By its combination of studies of H I emission and absorption in the local universe, ALFALFA will allow a robust estimate of the local H I cross section, as well as a measure of its clustering correlation amplitude and scale. In addition to H I line studies, the frequency range of the ALFALFA survey will also include, serendipitously, lines from OHMs arising from the nuclear molecular regions in merging galaxy systems. Approximately 100 such sources are known to date, half of which were discovered recently at Arecibo (e.g., Darling & Giovanelli 2002). Observations of OHMs hold the potential for tracing the merger history of the universe, since the sources are associated with merging galaxies. An essential tool in this exercise is the OHM luminosity function at low z. ALFALFA should detect several dozen additional OHMs in the redshift interval 0.16–0.25 and allow a more robust determination of the low-z OHM luminosity function than currently available.

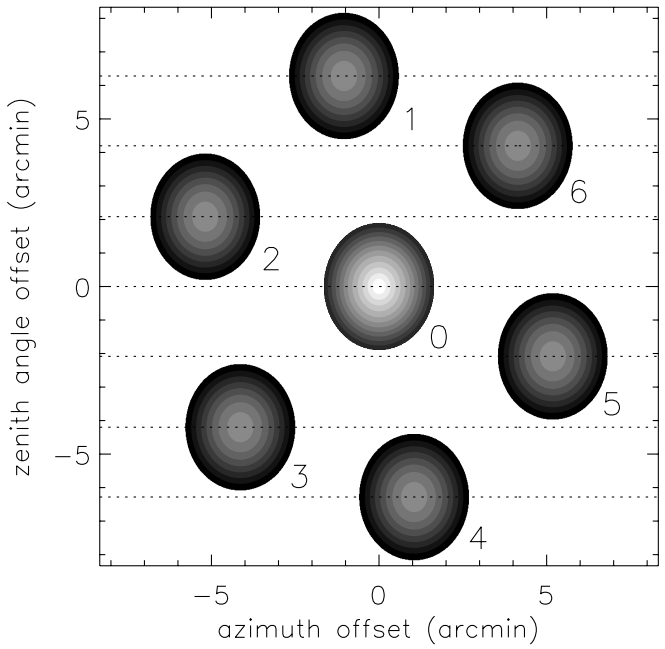

FIG. 2.—Sketch of the geometry of the ALFA footprint with the array located along the local meridian and rotated by an angle of 19° about its axis. The outer boundary of each beam corresponds to the −3 dB level. The dotted horizontal lines represent the tracks at constant declination of the seven ALFA beams as data are acquired in drift mode.

3. ALFA: THE ARECIBO L-BAND FEED ARRAY AND ITS SPECTRAL LINE BACK END

The construction of the Gregorian subreflector system for the Arecibo telescope, completed in the late 1990s, made possible the development of focal plane feed arrays (effectively, *creating* a focal plane). This development was foreseen during the planning phases of the Gregorian upgrade (Kildal et al. 1993). A seven-feed array was commissioned at the observatory during 2004. Six of the seven feeds (numbered 1–6) are physically arranged on the corners of a regular hexagon, while the seventh (feed 0) is at its center, as shown in Figure 2. The feeds can receive dual linear polarizations, and their spectral response is optimized for the range 1225–1525 MHz. They are stepped TE_{11} mode horns of 25 cm aperture, as described in Cortés-Medellín (2002). Because the optical design of the Gregorian subreflectors maximizes the illuminated area of the primary by sacrificing its circular symmetry (the illuminated area is elliptical), a circular pattern in the sky maps on the focal plane as an ellipse of axial ratio 1.15; reciprocally, the footprint of the centers of the outer beams of the ALFA array on the sky is that of a hexagon inscribed in an ellipse of that axial ratio. Similarly, the seven beams have an elliptical shape of the same axial ratio and orientation as the array pattern. The major axis of the ellipse is linked to the azimuth

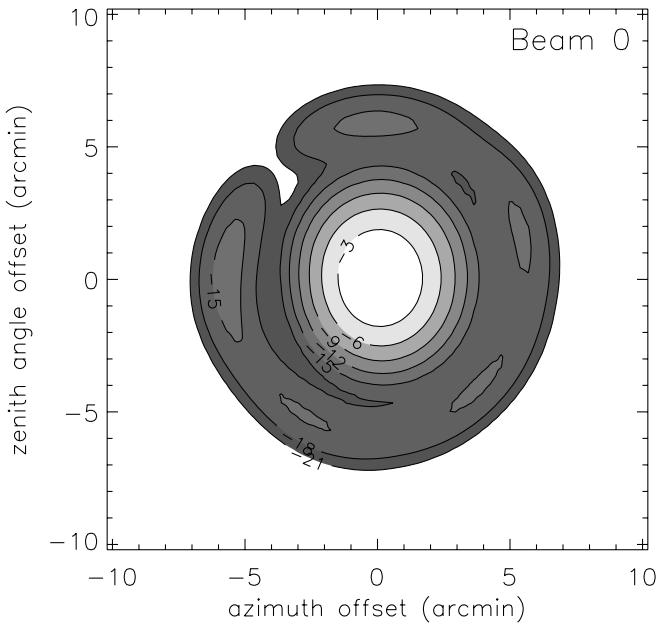

FIG. 3.—Beam pattern of beam 0. Contour lines and shading intervals are plotted at intervals of 3 dB below peak response (the highest contour is at half the peak power). The first sidelobe ring, with a diameter near 12′, is at approximately −15 dB.

of the receiver, so its orientation on the sky changes with telescope configuration. In Figure 2 the relative location of the beams is shown when the array is positioned at the meridian and rotated about its symmetry axis by 19°. In this sketch, the outlines of the beams are shown at the half-power response, for which the beam sizes are 3.′3 along the azimuth direction and 3.′8 along the zenith angle direction, with small variations from one beam to the other. The central beam 0 has higher gain ($\simeq$11 K Jy^{-1}) than the peripheral beams 1–6 (gain of $\simeq$8.5 K Jy^{-1}), which is illustrated in the sketch by the brighter contours. The dotted lines indicate the tracks of constant declination made by each of the beams when data are acquired in drift mode. Projected on the sky, the ALFA footprint in this configuration is such that beam 1 points farthest to the north and beam 2 farthest to the west for observations south of the zenith. For observations north of the zenith, beam 1 points farthest to the south and beam 2 farthest to the east.

Figures 3 and 4 show the pattern for each of the ALFA beams, obtained by mapping the radio source 3C 138 near transit. Sidelobe levels are very different for each of the beams of ALFA. Located at the center of the array, beam 0 has the most symmetric beam pattern, with a first sidelobe ring near 15 dB below the response at beam center, as shown in Figure 3. Contour levels are plotted at intervals of 3 dB. The outer beams have a very marked comatic aberration, as shown in Figure 4. The first sidelobe ring of the outer beams is strongly asymmetric, reaching levels near 7–8 dB below peak response, on the section away from the array center. This feature of the system will require careful attention, especially in the analysis of data obtained in the vicinity of strong and/or extended sources. The system temperature ranges between 26 and 30 K for all beam/polarization channels when pointing away from strong continuum sources.

The array can be rotated about its axis, centered on beam 0, and thus the relative position of the beams on the sky can be rotated along the elliptical perimeter. In the case of drift mode observations, it is desirable to position the array in such a manner that the beam tracks are equally spaced in declination. Because of the ellipticity of the array pattern on the sky, the separation between beam tracks depends on both the array rotation angle and the array azimuth. When the telescope feed arm is stationed along the local meridian, the optimal array rotation angle is 19°, as shown in Figure 2. In that case, beam tracks are spaced 2.′1 in declination. A single drift will thus sweep seven nearly equidistant tracks covering 14.′5 in declination at slightly below the Nyquist sampling rate. ALFALFA will map most of the extragalactic sky in drift mode with ALFA stationed along the local meridian at a local azimuth of either 0° (for observations south of zenith) or 180° (for north of zenith). Only declination tracks transiting within 2° of the zenith will be mapped with ALFA at an azimuth near 90° or 270° in order to avoid impractically small zenith angles. The beam separation for equidistant tracks is 1.′8 at these azimuths; thus, the declination sampling will be denser, as the elliptical pattern of the sky footprint of both the array and the individual beams will have its major axis oriented nearly parallel to the drift direction. Our survey will thus be done with ALFA in only two sets of configurations: one for all observations between declinations 0° and 16°, as well as between 20° and 36°, with ALFA on the meridian, and a second for observations between declinations 16° and 20°.

Spectra will be recorded every second, yielding approximately 14 samples per beam in the right ascension direction. This sampling rate, which greatly exceeds Nyquist, is principally motivated by the advantages derived from the identification of radio-frequency interference (RFI). Further details on ALFA can be found at the NAIC Web site.[29]

ALFALFA uses the feed array connected through a fiber optic intermediate frequency–local oscillator system to a spectral line, digital back end consisting of a set of processors, each individually referred to as a WAPP (Wideband Arecibo Pulsar Processor). The full spectral back end consists of four WAPP units, each capable of processing the two polarization signals from two ALFA beams. The WAPP set can thus produce 16 autocorrelation spectra, each with a maximum bandwidth of 100 MHz, over 4096 lags. Fourteen of those are matched to the seven polarization pairs from the ALFA beams, and a spare pair duplicates the signal of the seventh beam. At the offline processing stage, the extra pair of spectra is used for RFI monitoring purposes. Each data record thus consists of 65,536 spectral samples (16×4096). Since, as mentioned above, ALFALFA records data every second, the generation of raw data by the survey is slightly over 1 GB hr^{-1}, including headers.

4. SURVEY DESIGN

The strategy for the ALFALFA survey has been developed over the last few years, balancing the practical realities involved in using the Arecibo telescope, the constraints of telescope time availability, and the principal science objectives outlined in § 2. Here we review the considerations that enter into the survey design and numerical simulations that have been used to refine it.

4.1. *Scaling Relations*

The H I mass of an optically thin H I source at distance $D_{\rm Mpc}$, in solar units, is

$$M_{\rm H\,I}/M_{\odot} = 2.356 \times 10^5 D_{\rm Mpc}^2 \int S(V)\, dV, \qquad (1)$$

[29] See http://alfa.naic.edu.

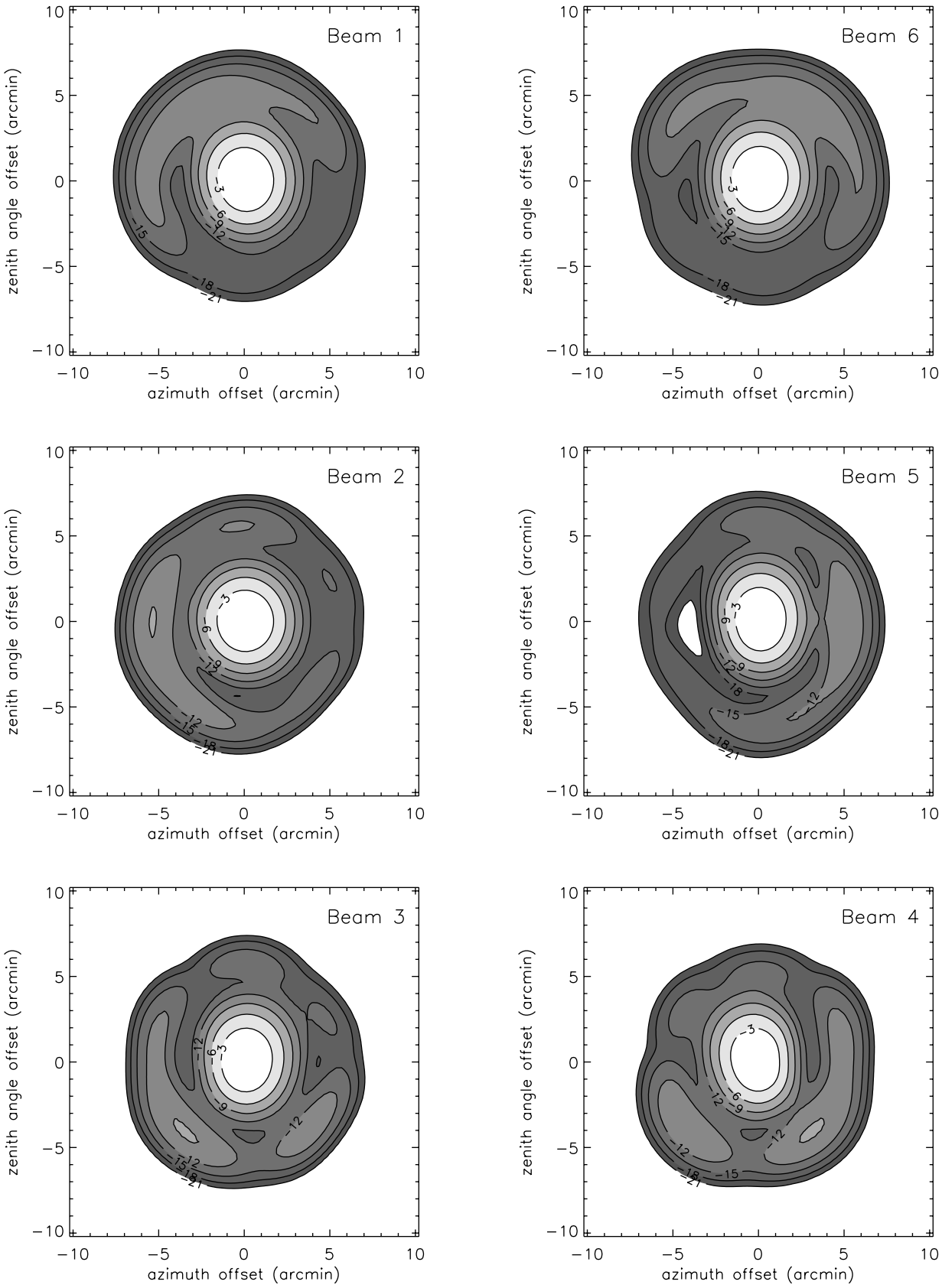

FIG. 4.—Beam patterns of the six peripheral ALFA beams. Contour lines and shading intervals are plotted at intervals of 3 dB below peak response (the highest contour is at half the peak power). Note that the sidelobe levels are significantly larger than for the central beam 0 and that they rise steeply on the outer side of the array, exhibiting strong comatic aberration.

where $S(V)$ is the H I line profile in janskys and V is the Doppler velocity in kilometers per second. To first order,

$$M_{\rm H\,I}/M_\odot \simeq 2.4\times10^5 D^2_{\rm Mpc} S_{\rm peak} W_{\rm km\,s^{-1}}, \quad (2)$$

where $S_{\rm peak}$ is the line peak flux and $W_{\rm km\,s^{-1}}$ its velocity width in kilometers per second. For detection, the signal-to-noise ratio (S/N) $s = f_\beta S_{\rm peak}/S_{\rm noise}$ must exceed some threshold value; $f_\beta \le 1$ quantifies the fraction of the source flux detected by the telescope's beam. The parameter $f_\beta = 1$ for a point source, while for resolved sources it decreases roughly like the ratio between the beam solid angle and the solid angle subtended by the source. An estimate of $S_{\rm noise}$ can be obtained from the radiometer equation for the rms value

$$S_{\rm rms} = \frac{(T_{\rm sys}/G)}{\sqrt{2\Delta f_{\rm ch} t_s f_t}}, \quad (3)$$

where $T_{\rm sys}/G$ is the system temperature divided by the system gain (for the ALFA feeds, $T_{\rm sys}/G$ will vary between 2.65 and 3.40 Jy; here we adopt a flat value of 3.25 Jy), $\Delta f_{\rm ch}$ is the channel bandwidth in hertz, and t_s is the integration time in seconds. The factor 2 under the square root indicates that two independent polarization channels are averaged. For ALFALFA, $\Delta f_{\rm ch} = 25$ kHz, which at the rest frequency of the H I line is equivalent to 5.3 km s^{-1}. The factor f_t accounts for spectral smoothing of the signal, $f_{\rm smo}$, the switching technique applied for bandpass subtraction, $f_{\rm switch}$, and other observational details, such as autocorrelation clipping losses; i.e., $f_t = f_{\rm switch} f_{\rm smo} f_{\rm other}$. For the data-taking scheme of ALFALFA, $f_{\rm switch} f_{\rm other} \simeq 0.7$. The S/N of a feature of width $W_{\rm km\,s^{-1}}$ is best rendered when the noise is measured after smoothing the signal to a spectral resolution on the order of $W_{\rm km\,s^{-1}}/2$. In practice, however, the smoothing of L-band spectra of $W_{\rm km\,s^{-1}} \simeq$ several hundred km s^{-1} does not reduce the noise in proportion to $W^{1/2}_{\rm km\,s^{-1}}$, and, moreover, $S_{\rm peak}$ is depressed by such smoothing, for spectral shapes are by no means boxlike. The fact that the detection criterion described above applies well to narrow lines but not so to wider ones was also noted by RS02. We assume here that spectral smoothing will increase S/N up to a maximum $W_{\rm km\,s^{-1}} \simeq 200$ and that smoothing beyond that width will be ineffective in increasing s. For a conservative S/N threshold of 6, we can then write

$$12.3 f_\beta t_s^{1/2} \left(\frac{M_{\rm H\,I}}{10^6\ M_\odot}\right) D^{-2}_{\rm Mpc} \left(\frac{W_{\rm km\,s^{-1}}}{200}\right)^\gamma > 6, \quad (4)$$

where $\gamma = -1/2$ for $W_{\rm km\,s^{-1}} < 200$ and $\gamma = -1$ for $W_{\rm km\,s^{-1}} \ge 200$. By inverting, we can obtain a minimum detectable H I mass:

$$\left(\frac{M_{\rm H\,I}}{10^6}\right)_{\rm min} = 0.49 f_\beta^{-1} D^2_{\rm Mpc} t_s^{-1/2} (W_{\rm km\,s^{-1}}/200)^{-\gamma}. \quad (5)$$

With an integration time of 30 s per pixel solid angle (see § 6) or 48 s per beam solid angle, ALFALFA should thus detect a H I mass of $10^6\ M_\odot$, $W_{\rm km\,s^{-1}} = 25$ at a distance of $\sim$6.5 Mpc and a source of $10^7\ M_\odot$ and of the same width out to $\sim$20 Mpc.

It is useful to review some of the basic scaling relations relevant to the design of a survey:

1. The minimum integration time required to detect a source of H I mass $M_{\rm H\,I}$ and width $W_{\rm km\,s^{-1}}$ at $s = 6$ at the distance $D_{\rm Mpc}$ with ALFA is, from equation (5),

$$t_s \simeq 0.023 f_\beta^{-2} \left(\frac{T_{\rm sys}}{G}\right)^2 \left(\frac{M_{\rm H\,I}}{10^6\ M_\odot}\right)^{-2} (D_{\rm Mpc})^4 \left(\frac{W_{\rm km\,s^{-1}}}{200}\right)^{-2\gamma}, \quad (6)$$

i.e., the depth of a survey increases only as $t_s^{1/4}$. With equality of back ends, the t_s required to detect a given $M_{\rm H\,I}$ at a given distance decreases as the square of G, i.e., as the fourth power of the reflector diameter. Arecibo offers a tremendous advantage because of its huge collecting area.

2. The beam of a telescope of collecting area A is $\Omega_b \propto A^{-1}$, while the maximum distance at which a given H I mass can be detected is $D_{\rm max} \propto G^{1/2}$. Since $G \propto A$, the volume sampled by one beam to the maximum distance $D_{\rm max}$ is $V_{\rm beam} \propto \Omega_b D^3_{\rm max}/3 \propto A^{1/2}$; i.e., in a fixed time, a radio telescope samples a volume that scales with the reflector diameter, yielding a significant comparative advantage for a large aperture like Arecibo.

3. Assuming that clouds of mass $M_{\rm H\,I}$ are randomly distributed in space out to the maximum distance at which they are detectable, $D_{\rm max}(M_{\rm H\,I})$, the number of clouds detected by a survey increases linearly with the sampled volume $V_{\rm survey} = \Omega_{\rm survey} D^3_{\rm max}/3$, where $\Omega_{\rm survey}$ is the solid angle mapped by the survey. We can thus increase the number of detections either by sampling a larger solid angle $\Omega_{\rm survey}$ or by increasing $D_{\rm max}(M_{\rm H\,I})$. Now, the total time required to complete the survey is

$$t_{\rm survey} \propto (\Omega_{\rm survey}/\Omega_b) t_s, \quad (7)$$

where Ω_b is the telescope beam. Since $D_{\rm max}(M_{\rm H\,I}) \propto t_s^{1/4}$, as shown in equation (6), we can write

$$V_{\rm survey}(M_{\rm H\,I}) \propto \Omega_{\rm survey} [D_{\rm max}(M_{\rm H\,I})]^3 \propto \Omega_{\rm survey} t_s^{3/4} \propto t_{\rm survey} t_s^{-1/4}, \quad (8)$$

and inverting,

$$t_{\rm survey} \propto V_{\rm survey}(M_{\rm H\,I}) D_{\rm max}(M_{\rm H\,I}) \propto V_{\rm survey}(M_{\rm H\,I}) t_s^{1/4}. \quad (9)$$

To achieve a given surveyed volume $V_{\rm survey}(M_{\rm H\,I})$, once $M_{\rm H\,I}$ is detectable at an astrophysically interesting distance, it is more advantageous to maximize Ω than to increase the depth of the survey $D_{\rm max}(M_{\rm H\,I})$.

The scaling relations described above provide only general guidelines in the design of a survey. Other considerations can and will play important roles in the survey strategy. For example, the growing impact of RFI on H I spectroscopy dictates increased attention to signal identification and corroboration, recommending a survey with more than a single pass over a given region of sky, as we discuss in § 5.2. The determination of specific properties of galaxies or systems may drive toward deeper surveys of narrow solid angle regions, as planned for other ALFA surveys with the Arecibo telescope, the goals and products of which will be complementary to ALFALFA.

4.2. *Survey Simulations*

The scaling relations described above dictate that ALFALFA cover a very large solid angle. In practice, the survey design

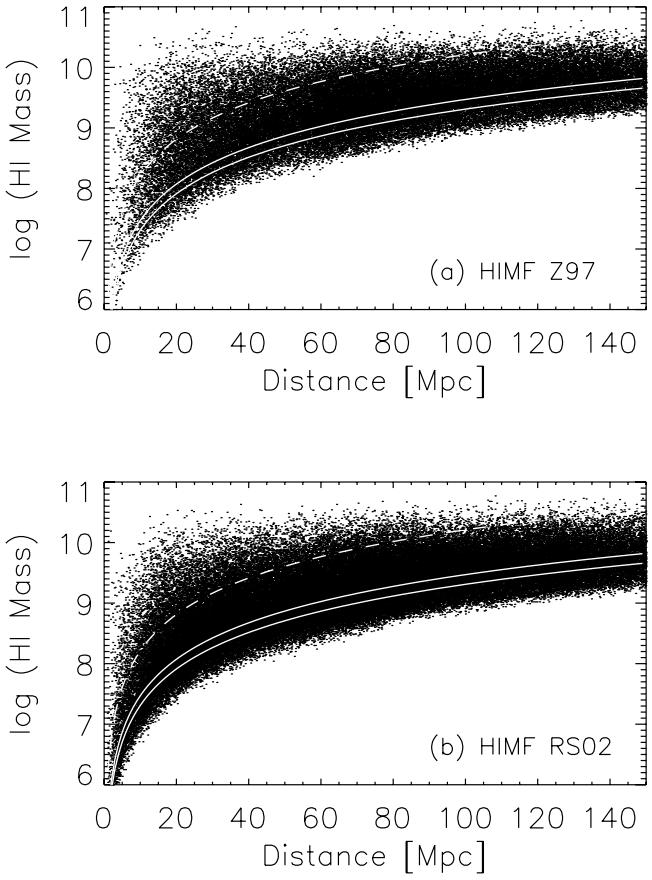

FIG. 5.—H I mass vs. distance of expected detections within $D < 150$ Mpc, assuming (*a*) a Z97 HIMF and (*b*) an RS02 HIMF. Calculations were made for the ALFALFA sky region specified in § 5.3, $t_s = 30$ s per map pixel area, and a detection threshold S/N = 6. The solid lines in both panels indicate detection limits of 0.9 and 1.25 Jy km s^{-1}. The first would be near the completeness limit of the survey for sources of width <200 km s^{-1}, the second near the completeness limit for objects of the same width but with $t_s = 14$ s integration. The dashed line in each panel corresponds to a flux density of 6.8 Jy km s^{-1}, a 6 σ HIPASS detection limit for a 200 km s^{-1} wide source.

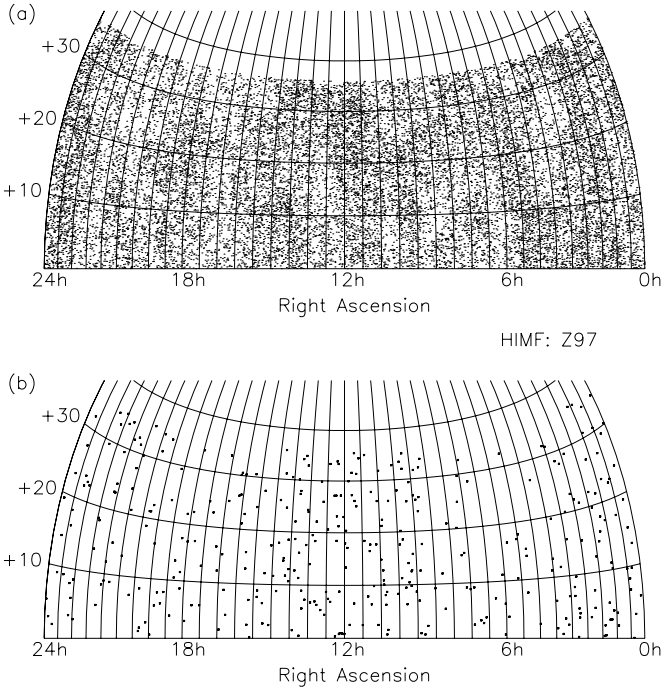

FIG. 6.—Sky distribution of expected detections for an ALFALFA-like survey as rendered with a Z97 HIMF. (*a*) Sources of all H I masses; (*b*) only those with $M_{\rm H\,I} < 10^8\ M_\odot$. Note that the ALFALFA survey will be restricted to R.A. = $07^{\rm h}$–$16^{\rm h}30^{\rm m}$ and $22^{\rm h}$–$3^{\rm h}$, although the full range of right ascension is shown in the figure.

must weigh the desire to cover a wide area with the need for sensitivity. An indispensable aid in the design of a survey is a thorough examination of expectations vis-à-vis variance over the survey parameter space. To this end, we have carried out an extensive set of survey simulations to help in the design of ALFALFA, and we present a sample of the results in this section.

The main ingredients for our survey simulation are (1) the survey mode and sensitivity parameters, derived from the instrument configuration; (2) an estimate of the space density of sources given by an adopted HIMF; and (3) an understanding of the clustering properties and deviations from smooth Hubble flow in the local universe. Sensitivity considerations were presented in § 4.1. For the HIMF, we use two recent estimates that differ strongly from each other at the low-mass end: that of Z97 and that of RS02. The more recent HIMFs by Z04 and Springob et al. (2005a) are bracketed by those of Z97 and RS02. We use a density map of the local universe provided by Branchini et al. (1999), which is a density reconstruction derived from the Point Source Catalog Redshift Survey (PSCz). The grid we used has a spacing of 0.9375 h^{-1} Mpc in the inner 60 h^{-1} Mpc and a spacing twice that value between 60 and 120 h^{-1} Mpc, where $h = 0.7$; the map is smoothed with a Gaussian filter of $\sigma = 3.2\ h^{-1}$ Mpc. For distances larger than 120 h^{-1} Mpc, we assume a constant density.

Sources are seeded using the density map and, separately, each of the two HIMFs. The H I gas is assumed to be optically thin. Because many of the sources will be resolved by the Arecibo beam, an estimate of H I size is necessary. Assuming that the H I distribution is disklike, inclinations to the line of sight and line widths need to be assigned to each source. We use empirical scaling relations obtained from our own H I survey data (Springob et al. 2005b) and Broeils & Rhee (1997), and we add random inclinations, realistic scatter, and broadband spectral baseline instability. With these recipes, we have inspected a wide grid of survey parameters in arriving at the adopted ALFALFA survey strategy.

As an example, Figure 5 displays the variation with distance of the H I mass of expected detections within the region of the ALFALFA sky coverage, as described in § 5.3, adopting as input the two different HIMFs: that of Z97 (Fig. 5*a*) and that of RS02 (Fig. 5*b*). Only expected detections out to 150 Mpc are shown. The simulation corresponds to an integration time $t_s =$ 30 s per map pixel solid angle. The number of detections expected with RS02 is 22,200, while the number expected with Z97 is 15,022, with a detection threshold of S/N = 6, as defined in § 4.1. The difference in expected detections is more dramatic when the H I mass of the source is restricted to $M_{\rm H\,I} < 10^8\ M_\odot$. In that case, we expect 1400 detections with RS02 and only 249 with Z97. It is interesting to point out that in the course of ALFALFA precursor observations, reported in Paper II, three objects with $M_{\rm H\,I} < 10^7\ M_\odot$ were detected. Albeit of still marginal statistical value, that rate is consistent with the high end of the expectations (RS02 HIMF) obtained from the simulations reported here.

Three curves are shown in each panel of Figure 5. The two solid lines are the loci of constant integrated H I line flux of 0.9 and 1.25 Jy km s^{-1}. The lower of the two corresponds to the

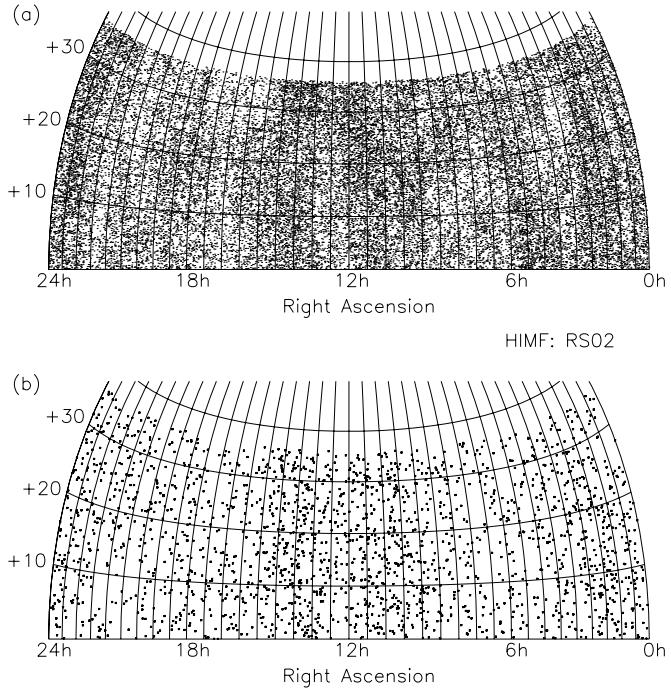

FIG. 7.—Same as Fig. 6, except that the RS02 HIMF was used for the simulation.

completeness limit of the survey for sources of $W_{\mathrm{km\,s^{-1}}} \leq 200$ (detections below that line correspond to sources of smaller width). The second curve corresponds to the completeness limit for sources of the same width, for an integration time per pixel of $t_s = 14$ s. Such an integration time applies to the analysis of individual drift tracks, without the corroborating support (and higher resulting integration) of spectra in beam tracks at neighboring declinations. This detection limit would result if source extraction were carried out, for example, right after data taking and before an entire data cube (spatially two-dimensional, plus one spectral dimension) is available. In this case, the expected number of detections would be 13,804 for the RS02 HIMF and 9601 for the Z97 case, a drop of 38% and 36%, respectively, from the previous set of numbers. The decrease in the number of detections with small H I masses would be more severe if signal extraction were applied to individual tracks only, rather than to full maps; in that case, only fewer than half of the sources would be detected in the RS02 case and just above half in the Z97 case.

The dashed curve in Figure 5 corresponds to a flux integral of 6.8 Jy km s^{-1}, the HIPASS completeness limit at the 6 σ level, for detection of sources of width $\leq$200 km s^{-1}; this is the HIPASS analog of the lower of the two solid lines for ALFALFA. It uses a HIPASS limit of 13.3 mJy per map pixel area, as reported by Barnes et al. (2001). This provides a good graphical illustration of the comparison between the two surveys.

Figure 6 shows the sky distribution of the detected sources by an ALFALFA-like survey in the simulation with the Z97 HIMF. Sources at all right ascensions are plotted, albeit ALFALFA will only cover 60% of the full right ascension range. In Figure 6*b*, only the detections with $M_{\mathrm{H\,I}} < 10^8\,M_\odot$ are plotted. Figure 7 shows the analogous graphs for the RS02 HIMF.

Simulation results such as those presented here aid us in the estimate of the statistical efficacy of the survey data, most importantly in the determination of the faint end of the HIMFs and the clustering properties of the new detections.

5. OBSERVING MODE

Given the science objectives outlined in § 2 and the scaling relations and simulations presented in § 4, the final consideration of the survey design strategy takes into account more telescope-related practicalities. In this section, we review those issues that have led us to adopt a very simple observing strategy, a two-pass drift scan mode, covering the sky with "tiles" in the range $0^\circ <$ decl. $< +36^\circ$.

5.1. *Drift Mode*

The Arecibo telescope is an altitude-azimuth system located at a latitude near 18°. Its Gregorian dome can be steered within $\sim$20° of the zenith, but the system gain and performance degrades rapidly at zenith angles above $\sim$18°. In general, the performance characteristics, including beamwidth, pointing accuracy, sidelobe levels, spectral baseline stability, and susceptibility to RFI, vary with azimuth, zenith angle, and feed rotation angle. Furthermore, the ALFA footprint on the sky and its beams' structure likewise vary in a complicated manner. The design of ALFA surveys is thus strongly constrained by this variance, and with it, the corresponding degree of calibration complexity a particular observing program can endure. ALFALFA aims to minimize the impact of these factors on performance through a choice of maximum simplicity in the observing mode and minimal electronic intrusion at the detection level.

As mentioned in § 3, the ALFALFA survey is thus being carried out in a fixed azimuth drift mode. For most of the survey, the azimuth arm of the telescope is stationed along the local meridian, the zenith angle of ALFA determining the declination to be mapped. A tiny elevation readjustment is periodically applied to maintain drift tracks at constant J2000.0, rather than current declination. Without such adjustment, drift tracks taken a few years apart would noticeably diverge from one another. No firing of noise calibration diodes is done during normal data acquisition. Rather, data taking is interrupted very briefly every 10 minutes while a calibration noise diode is fired for 1 s. This interruption produces data gaps of 5 s—approximately one-third of a beamwidth in right ascension—in each 600 s drift data stream. The central frequency of the bandpass is set and never changed during an observing session; i.e., no Doppler tracking of the local oscillator frequency is applied. (Realignment to a common heliocentric reference frame is applied to each spectrum offline, using high-precision time, position, and Earth's motion stamps updated every second in data headers.) With no moving telescope parts, constant gain and nearly constant system temperature along a drift are obtained; standing waves change slowly, as driven by the sidereal rate; beam characteristics remain fixed; and bandpass subtraction is optimized.

The solid angle mapped by the survey is subdivided into tiles of 4° in declination (see below and Fig. 1) extending from decl. = 0° to 36°. For eight of the nine bands of tiles, the azimuth of the feed array is along the local meridian (at azimuth either 0° or 180°), while the rotation angle of the feed array is fixed at 19°, yielding tracks for the seven array beams that are equally spaced in declination. In order to map the telescope's zone of avoidance near zenith, the band of tiles centered at decl. = +18° will require a different orientation: with the azimuth arm nearly east-west. This strategy greatly simplifies the disentangling of main beam and sidelobe contributions to the maps; characterization of ALFA parameters thus needs to be made on a greatly reduced volume of telescope configuration parameter space.

Drift mode observations, combined with the calibration scheme described above, yield maximally efficient use of telescope time,

providing high photometric quality with very small overhead. We expect that, barring instrumental malfunctions, telescope time usage for science data will approach 97%.

5.2. *Two-Pass Strategy*

As discussed in § 4.1, the volume sampled at any H I mass limit for a survey of fixed total duration varies with the integration time per point as $t_s^{-1/4}$. Once a threshold sensitivity is reached, it is more advantageous to increase the solid angle of the survey than its depth. Because of the spacing of the ALFA beam tracks in drift mode discussed in § 3, coverage of the sky in a one-pass drift survey is slightly worse than Nyquist. For a fixed amount of observing time, a single-pass strategy would appear to maximize the number of detected sources. For a fixed total survey time, the loss of survey volume sampled by going from a one-pass to a two-pass drift survey is, according to § 4.1, 19%. Several advantages of a two-pass strategy offset that loss, however: (1) A second pass will greatly aid the separation of cosmic emission from RFI, which is unlikely to affect each pass identically. (2) The denser sky sampling will allow statistical separation of spurious signals from cosmic ones, thus allowing reliable detection to lower values of S/N. (3) If the two passes are made when Earth is at very different phases of its orbit, confirmation of cosmic nature for detection candidates can be obtained by verifying that they are separated in topocentric radial velocity by $30 \cos(\Delta\theta)$ km s^{-1}, where $\Delta\theta$ is the change in the angle between the line of sight to the detection candidate and the velocity vector of Earth on its heliocentric orbit; this requires that the second pass be undertaken 3–9 months after the first pass, modulo 1 yr. (4) The variability of radio continuum sources can be measured, and radio transients can be identified, allowing commensality with other science teams interested in studies of those phenomena. (5) Given the design features of the ALFA hardware, maintenance will be difficult, and, as a result, ALFA may operate at less than 100% capacity (i.e., one or more beams may be unusable) during some fraction of the time. Loss of a beam in a single-pass survey would result in grievous holes in sky coverage, whereas a two-pass strategy would greatly attenuate the resulting damage to the survey. For all these reasons, the high Galactic latitude Arecibo sky to be mapped by ALFALFA will be covered in two drift passes. The resulting effective integration time of the survey per beam area will be about 48 s. Another way of expressing the sensitivity of the survey is in terms of the integration time per square degree, which will be about 14,700 s.

5.3. *Sky Tiling and Data Products*

As shown in Figure 1, the sky to be mapped by ALFALFA extends over the range $0^\circ <$ decl. $< 36^\circ$ and over two blocks of right ascension, 07^h30^m–16^h30^m and 22^h00^m–03^h00^m, although the vagaries of telescope time allocation will produce some irregularities in the survey solid-angle boundaries. The exclusion of the low Galactic latitude regions within the telescope's horizon is driven by (1) the realistic assessment that pulsar and other Galactic ALFA surveys will greatly increase the pressure on low Galactic latitude local sidereal times and (2) the expectation that part of the low Galactic latitude, extragalactic sky will be surveyed commensally with pulsar and other Galactic surveys.

For bookkeeping and data release purposes, the sky mapped by ALFALFA will be subdivided into 378 tiles, each of R.A. $= 20^m$, decl. $= 4^\circ$. Mapping a tile in single-pass drift mode requires 17 drifts of ALFA, spaced $\sim 14'$ in declination and each yielding seven drift tracks; equally as many additional drifts are required to complete the second pass at a later time. For the second pass, beam tracks will be interleaved with those of the first pass, so that the final declination sampling will be $\sim 1'$, better than Nyquist. In order to minimize "scalloping" of the gain over the map introduced by the higher gain of the central beam relative to the outer ones, the second-pass drifts are offset by $7'18''$ relative to the first-pass tracks.

The data processing environment chosen for ALFALFA is IDL. A substantial body of spectral line software generated by one of us (P. P.) already exists at the Arecibo Observatory. Further development specific to ALFALFA has been grafted onto this fertile base. The tile size was chosen to constitute a data block that can reasonably be handled for data processing in an efficient manner by current desktop computers. The generation of raw data proceeds at the rate of ~ 1.2 GB hr^{-1}, and, on conversion from its raw FITS format to an IDL structure, a single 600 s drift is ~ 200 MB. Such a data block is well suited for one of the most computer-intensive parts of the reduction pipeline, that of bandpass subtraction. The data for a full tile, after polarization averaging and regridding, can fit within the 2–4 GB memory of current low-cost desktops.

The data processing path for ALFALFA data can be summarized as follows:

1. One FITS file per 600 record drift is generated by the data-taking software at the Arecibo Observatory. By the end of each observing session, each of those is converted into an IDL structure, which we refer to as a "drift" structure, and stored for further analysis at the observatory and the observers' institutions.
2. Within weeks, all data of an observing session are noise-calibrated, and a bandpass solution is computed. The bandpassed, calibrated, and baselined spectral data for each beam/polarization configuration are obtained as output of an automated pipeline that is designed to preserve not only small angular scale features such as external galaxies but also large structures such as HVCs and Galactic H I.
3. The first detailed visual inspection of the data follows, in the course of which the observer flags regions of each position-velocity map for RFI and other occurrences of data corruption. It is anticipated that as much as about half of all sources to be detected by ALFALFA will be visible to the eye at this stage. A first automated signal extraction algorithm pass produces a list of candidate detections. Noise diode–calibrated, bandpass-corrected, baselined, and RFI-flagged spectra as obtained at this stage constitute what we refer to as "Level I Data Products."
4. On completion of the second pass through a given sky tile, data are recalibrated using the continuum sources present within the tile, regridding of the sky sampling takes place after smoothing by a homogeneous resolution kernel, and conversion into data cubes follows. The output of this processing stage is referred to as "Level II Data Products."

Because telescope scheduling is a dynamic process that responds to proposal pressure at a national center, the scheduling of data releases far in advance is not possible. However, the ALFALFA observing status is continuously updated at the survey Web site.[30] Observing plans foresee completion by bands of tiles, and, when an accurate prediction of the completion is available, data release plans for that band will be posted. Data release will take place through an ALFALFA H I node connected to the US National Virtual Observatory. A preliminary example of Web-based data presentation is linked to the aforementioned Web site,

[30] See http://egg.astro.cornell.edu/alfalfa.

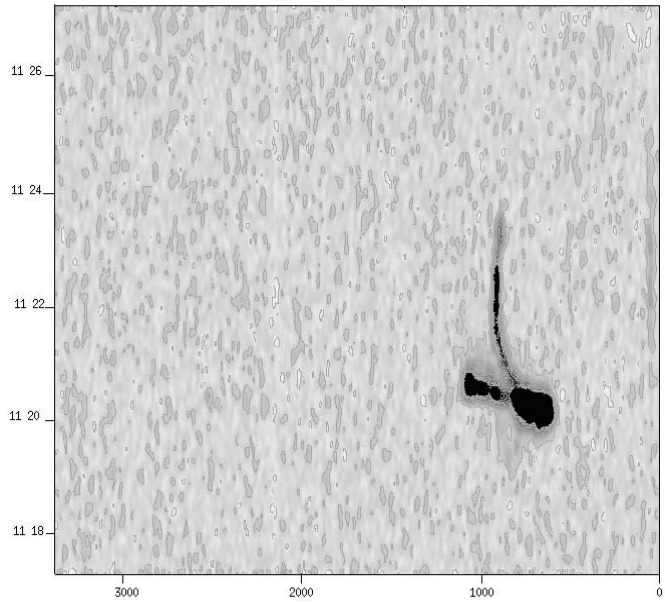

FIG. 8.—Position-velocity map cutting across NGC 3628 and its tidal tail at constant decl. (J2000.0) = +13°36′45″. The lowest contour is at 2 mJy beam^{-1}, and other contours are spaced by 6 mJy beam^{-1}. See text in § 5.3 for further details.

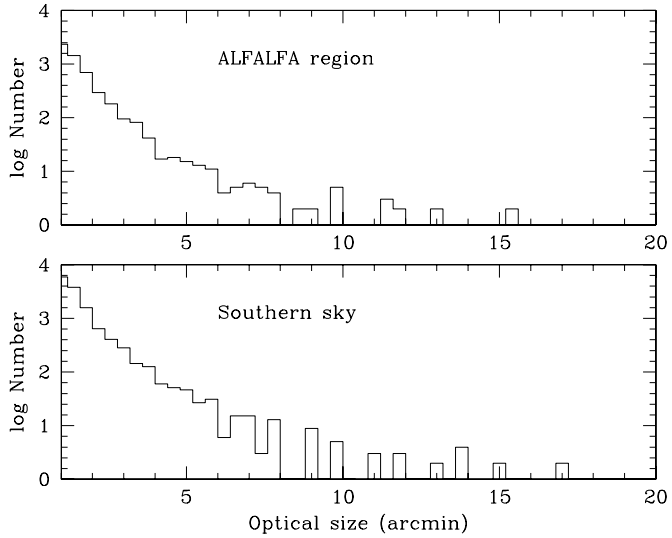

FIG. 9.—Histograms of the optical major blue diameter, D_{25}, of galaxies larger than 1′ in the ALFALFA survey region (*top*) and the whole southern hemisphere (*bottom*). Aperture synthesis studies have shown that the diameter of the H I disk for optically selected galaxies is, on average, 1.6 times larger than the optical size. The Parkes 15′ beam thus resolves on the order of 15 galaxies over the whole southern hemisphere; the ALFA ∼3.′5 beam should resolve several hundred galaxies over the ALFALFA survey region. The bin size is 0.′1 in both histograms.

as well as directly reachable;[31] it allows access to the spectral line data, images of optical counterparts, and parameter tabulation of the precursor observations' results, which are discussed in Paper II.

As an example of a Level I Data Product and the potential of the ALFALFA survey, Figure 8 shows a single-pass drift across the galaxy NGC 3628, one of the Leo triplet galaxies, and its tidal tail. The displayed position-velocity image consists of a constant declination drift of 600 1 s records at decl. (J2000.0) = +13°36′45″, corresponding to decl. (B1950.0) = +13°53′09″, for comparison with Figure 1 of Haynes et al. (1979). The single-drift rms noise in the image is 3.5 mJy. Contours are linearly spaced by 6 mJy, and the lowest contour is plotted at 2 mJy beam^{-1}. The tidal tail is traced by the ALFALFA data as far as the earlier point-by-point map, but a countertail at earlier right ascension than NGC 3628 is also clearly visible in the new map. After the second-pass ALFALFA data become available, the Leo triplet region will be mapped with a sensitivity twice as deep as that shown in Figure 8, allowing a detailed study of the system over a wide area.

6. EXPECTED SURVEY SENSITIVITY

Here we summarize the sensitivity of ALFALFA at several survey levels:

1. A 1 s record of a drift scan, after accumulation of both polarizations, will yield a spectrum of $S_{\rm rms} \simeq 13(\mathrm{res}/10)^{-1/2}$ mJy, where res is the spectral resolution in kilometers per second.
2. A single-drift, position-frequency map spatially smoothed to the spatial resolution of the telescope beam will yield $S_{\rm rms} \simeq 3.5(\mathrm{res}/10)^{-1/2}$ mJy.
3. A spatially two-dimensional map of two-pass ALFALFA data, smoothed with a kernel of 2′ at half-power, will have $S_{\rm rms} \simeq 2.3(\mathrm{res}/10)^{-1/2}$ mJy pixel^{-1}.
4. The rms sensitivity per beam area after a two-pass survey will be $S_{\rm rms} \simeq 1.8(\mathrm{res}/10)^{-1/2}$.
5. The 6 σ H I column density limit will be $N_{\rm H\,I,lim} = 1.6 \times 10^{18}(W/10)(\mathrm{res}/10)^{-1/2}$ atoms cm^{-2} for a spectral line of width W km s^{-1} observed with a spectral resolution of res kilometers per second.

Column density sensitivity is, in general, independent of telescope size; thus, ALFALFA will not reach deeper $N_{\rm H\,I}$ levels than previous wide-angle surveys such as HIPASS. In fact, given the shorter integration time per beam area, ALFALFA will have lower sensitivity to $N_{\rm H\,I}$ than did HIPASS for very extended sources. It may be argued that only surveys with longer integration times per beam area than HIPASS can break new ground. However, this argument holds true only if sources are well resolved by the telescope beam. The beam area of Arecibo is nearly *20 times smaller* than that of the Parkes telescope. If sources are unresolved by the beam, the telescope can only detect total flux, and the observation cannot be used for any inference on source column density. In fact, very few extragalactic H I sources were resolved by the Parkes beam; the smaller Arecibo beam size gives ALFALFA a major advantage. To illustrate this point, Figure 9 shows two histograms of the angular size distribution of optically selected, cataloged galaxies: the top one for galaxies known to be within the ALFALFA survey region, the bottom one for galaxies in the whole of the southern hemisphere. The optical size used for this comparison is D_{25}, as cataloged in the Third Reference Catalogue of Bright Galaxies (de Vaucouleurs et al. 1991). It is well established that, on average, the H I size (measured at the level near 1 $M_\odot$ pc^{-2}) of optically selected galaxies is about 1.6 times that of the blue size (Broeils & Rhee 1997), although for dwarf irregular systems that ratio may rise significantly (Swaters et al. 2002). Even allowing for a small number of extremely large H I-to-optical size ratios, the total number of galaxies resolved by the Parkes telescope beam over the whole of the southern sky is on the order of one or two dozen. Only for those galaxies, the Magellanic Stream,

[31] At http://egg.astro.cornell.edu/precursor.

and HVCs is column density sensitivity of any relevance for HIPASS. The ALFALFA survey should, on the other hand, resolve several hundred galaxies and HVCs and map their peripheries to a column density limit on the order of 5×10^{18} atoms cm^{-2}. Through careful analysis of the H I mapping data sets, including consideration of the impact of sidelobe contamination in the two or three selected telescope configurations adopted for the drift survey, the ALFALFA survey will address the issue of whether a column density regime below 10^{19} cm^{-2} is commonly found in the local universe (Corbelli & Bandiera 2002).

7. CANDIDATE DETECTIONS AND VERIFICATION OF COSMIC SIGNALS

ALFALFA will produce a catalog of tens of thousands of candidate detections; on the order of 20,000 will be cosmic sources. The number of candidate detections per bin of S/N s will increase steeply, and the probability that the candidates are real sources will decrease rapidly with diminishing s value.

Internal (i.e., within the survey data set) corroboration of candidate detections will rely on (1) comparison of independent polarization samples and (2) comparison of spatially adjacent survey samples. The effectiveness of item (1) will depend on the spatial sampling density and, in the case of multiple drifts through the same region, on the temporal consistency of the data. These comparisons will help exclude many marginal candidate detections of noncosmic origin, which we shall refer to as "false" candidates.

Postsurvey, corroborating observations will be desirable to confirm candidate detections just below the S/N threshold above which signal corroboration can be internally possible. This may allow significant expansion of the survey "catch" with modest additional amounts of telescope time. The usual compromise is necessary in setting an s threshold: too high a threshold will lose many valuable potential detections, too low a threshold will require impractical amounts of postsurvey telescope time, and a haphazard criterion may corrupt the completeness of acquired samples.

We expect that the bulk of follow-up observations to corroborate the cosmic nature of detection candidates will be carried out at Arecibo using a single-pixel feed, hopping from one candidate to the next, and minimizing slew and setup time. Two modes may lead to low-efficiency usage of telescope time: too dense a set of follow-up targets may be comprised of too large a fraction of false candidates and thus produce a low yield per unit of telescope time, and too sparse a set may lead to a large fraction of the time spent slewing and in other overhead. Careful optimization will be required. We consider some of these issues in this section.

7.1. *Types and Numbers of Candidate Detections*

Visual inspection or automated signal extraction algorithms identify detection candidates that can be assigned to three classes: (1) cosmic sources, (2) extreme statistical fluctuations of noise, and (3) spurious signals due to RFI or other instrumental and data analysis causes.

Cosmic sources.—Figure 10 shows a histogram of S/N s of expected sources, as obtained in one of the simulations described in § 4.2. We emphasize that the number of sources rises steeply as s decreases, illustrating the well-known fact that most of the survey candidate detections will occur near the detection limit.

Because of the massive bulk of ALFALFA data sets, signal extraction will largely rely on automated procedures. A. Saintonge has coded a matched-filter, cross-correlation signal extraction algorithm, described elsewhere (A. Saintonge et al. 2005, in preparation). Detection probability simulations have been carried out with this algorithm by randomly injecting a Gaussian signal in simulated spectra with Gaussian noise and monitoring the effectiveness of the signal extraction algorithm in recovering the injected signal. The detection probability is computed as the fraction of all trials in which the signal extraction algorithm positively identifies the injected signal; such a probability is monitored as a function of s and of signal width. When the noise is measured after spectrally averaging over half the spectral width of the injected signal, the detection probability is largely independent of the signal width.

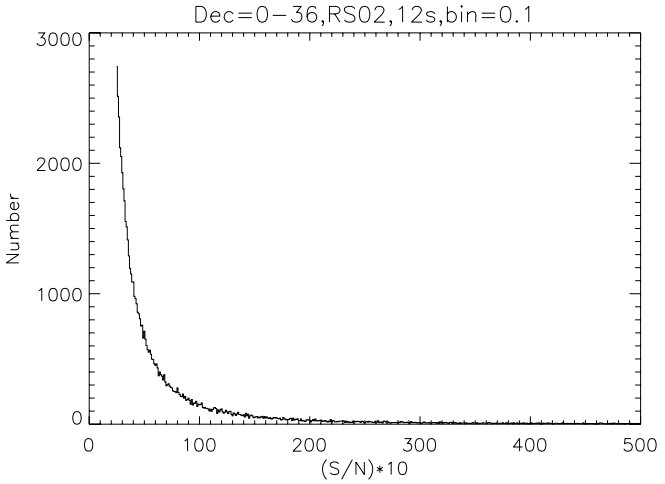

FIG. 10.—S/N histogram of a 12 s ALFALFA survey using the RS02 HIMF. S/N bins have a width of 0.1. S/N is defined as the peak signal flux to the rms computed in matched filter mode over a spectral resolution equal to half the signal width. Only tentative detections with S/N > 2.5 are plotted.

Statistical noise fluctuations.—For Gaussian noise, the probability that a single spectral channel yields a fluctuation of S/N between s_1 and $s_1 + ds_1$ is

$$p_1\, ds_1 = \frac{1}{\sqrt{2\pi}} e^{-s_1^2/2}\, ds_1, \tag{10}$$

where $s_1 = S_{\rm peak}/\sigma_1$, $S_{\rm peak}$ is the peak flux density, and σ_1 is the rms noise with single-channel spectral resolution. Similarly, the probability for an n_w channels wide spectral feature to exhibit a deviation between s_n and $s_n + ds_n$ is

$$p_n\, ds_n = \frac{1}{\sqrt{2\pi}} e^{-s_n^2/2}\, ds_n, \tag{11}$$

where $s_n = s_1/(n_w/2)^{1/2}$.

In a survey of $N_{\rm los}$ line-of-sight samples taken with a spectrometer of N_c channels, the number of samples n_w channels wide with S/N between s and $s + ds$ is

$$n_{s,n_w}\, ds = N_{\rm los} \frac{N_c}{n_w} p_n\, ds = N_{\rm los} \frac{N_c}{n_w} \frac{1}{\sqrt{2\pi}} e^{-s^2/2}\, ds, \tag{12}$$

and the total number of statistical fluctuations of that width with s larger than a threshold $s_{\rm th}$ is

$$N_{s_{\rm th},1} = N_{\rm los} \frac{N_c}{n_w} \frac{1}{\sqrt{2\pi}} \int_{s_{\rm th}}^{\infty} e^{-s^2/2}\, ds = N_{\rm los} \frac{N_c}{n_w} [F(\infty) - F(s)], \tag{13}$$

where, again, the noise is computed with a spectral resolution of $n_w/2$ channels and $F(s)$ is the familiar cumulative distribution of the normal error function: $F(-\infty) = 0$, $F(\infty) = 1$, and $F(0) = 0.5$. The total number of purely statistical noise fluctuations between s_a and s_b, with widths between n_{w1} and n_{w2}, appearing in the survey will then be

$$N_{[a,b],[1,2]} = \sum_{n_w=n_{w1},\,n_{w2}} N_{\rm los}\frac{N_c}{n_w}[F(s_a) - F(s_b)]. \qquad (14)$$

To first order, and ignoring the fact that, in the expression above, a high-s, broad feature gets overcounted as several lower s, narrower ones, we can approximate

$$N_{[a,b],[1,2]} \simeq N_{\rm los}N_c \ln\frac{n_{w2}}{n_{w1}}[F(s_a) - F(s_b)]. \qquad (15)$$

For example, for a survey that samples 10^7 lines of sight with a spectrometer usefully covering 85 MHz with $N_c = 3600$ spectral channels (so that a velocity width range between 25 and 500 km s^{-1} translates into $n_{w1} \simeq 5$ and $n_{w2} \simeq 100$), one should expect $N_{>3} \sim 2\times10^8$ features with $s > 3$, $N_{>4} = 5\times10^6$ features with $s > 4$, and $N_{>5} = 5\times10^4$ features with $s > 5$, with width anywhere between 25 and 500 km s^{-1}. These are ominously large numbers when compared to expected numbers of cosmic sources between 10^4 and 3×10^4 for that range of s.

RFI or other spurious signals.—The above assumption of Gaussian noise is heuristic. The true nature of the noise will be ascertained after a significant fraction of the survey data have been collected and the normal characteristics of both equipment and RFI environment have been measured. As we discuss in Paper II, the precursor observations carried out in 2004 were taken in commissioning mode for the ALFA hardware, and several internal bugs have been found and fixed since those observations were completed. Those observations are not well suited for a careful analysis of the problem. For the moment, we ignore the impact of RFI and other non-Gaussian sources of noise and restrict our analysis to the discrimination between cosmic sources and Gaussian noise fluctuations.

7.2. *Discriminating among Candidate Detections*

Assuming that the majority of weak detection candidates will be unresolved by the telescope beam, the most important means of discriminating between cosmic sources and noise fluctuations will result from comparison of contiguous drift tracks and different polarizations of the same beam. Consider a single-pass ALFALFA survey, whereby contiguous drift tracks are separated by 2.′1 in declination on the sky. A point source swept by one of the feeds will also appear in contiguous tracks at lower s. For an ALFA beam averaging 3.′5 width at half-power, the response 2.′1 off the beam center is about 0.37 of that on the beam center. In a two-pass drift survey, the track separations are 1.′05, and at that distance from the beam center, the beam response is 0.78 of that on the beam center. A point source will thus be far more easily confirmed in a two-pass survey. Similarly, since the H I line is unpolarized, the comparison of the two independent polarization spectra of the same beam will deliver equal signals, plus noise, for cosmic sources and completely uncorrelated results for noise. We refer to the exclusion of detection candidates made possible by comparison of adjacent drift tracks and polarization channels as "vicinity trimming"

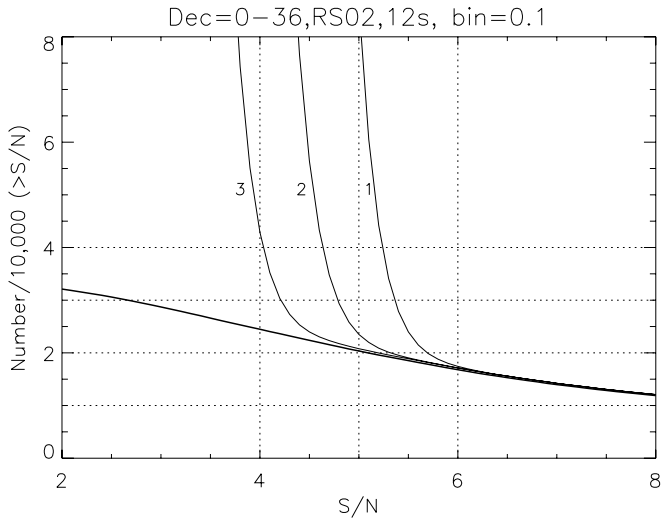

FIG. 11.—Cumulative number of candidate detections as a function of S/N expected for an all-Arecibo sky drift survey. The nearly horizontal line refers to the real sources (assuming an RS02 HIMF); the nearly vertical curves refer to the three cases of vicinity trimming described in § 7.2.

and distinguish three sets of detection candidates: (1) that obtained without any vicinity trimming, (2) that obtained after vicinity trimming in a single-pass survey, and (3) that obtained after vicinity trimming in a double-pass survey. The latter two sets are smaller than the first.

Figure 11 displays the cumulative number of candidate detections plotted as a function of S/N expected for an ALFALFA-like survey. The simulation assumes an RS02 HIMF and a sensitivity corresponding to a double-pass drift survey. The nearly horizontal line corresponds to the detection candidates associated with cosmic (real) sources. The three nearly vertical curves correspond to the expected number of noise fluctuations with the given s in the three vicinity trimming cases described above. At $s > 6$, most of the detection candidates are cosmic sources. At $s \simeq 5$, the number of real cosmic sources is 25% higher than at $s = 6$, but the candidate detections resulting from noise fluctuations can be several times higher than those of real sources. Vicinity trimming can, however, drastically reduce the number of candidate detections deserving attention. Only at S/N levels $s < 4$ does the number of noise fluctuations overwhelm that of cosmic sources after two-pass vicinity trimming. At this level, however, the impact of low power level RFI will play an important and yet quantitatively unknown role.

7.3. *Follow-up, Corroborating Observations*

Candidate detections with a comfortably high S/N threshold $s_{\rm th}$ will not need corroborating follow-up observations in order to confirm their reality as cosmic sources. Without considering the impact of RFI, $s_{\rm th}$ may be in the vicinity of 6; consideration of the impact of RFI may raise $s_{\rm th}$ to higher values in a variable manner, depending on the frequency of the candidate signal. Candidates with $s \simeq s_{\rm th}$ or slightly below that level will be reobserved with the Arecibo telescope. To how low a level of s should reobservations be considered? A simple criterion would be that corroborating observations should be requested only for candidates of s such that the expectation of confirmation, expressed in terms of detections per unit of telescope time, is at least as high as for the full survey.

If a corroborating observation is to require an increase in s from a value of, say, 5 for the survey data to about 7 for the

corroborating observation, integration times of at least 1 minute per candidate will be necessary for corroborating observations. Observing runs to corroborate several hundred candidate detections at a time will thus be the norm. If the set of candidate detections to be checked is very sparse—say, one candidate every several square degrees—slew times will be very substantial, and bandpass-correcting observations will be required for each candidate source, more than doubling the required telescope time. In that case, the on-source $t_{\rm int}$ of the order of 1 minute may be a small fraction of the overall time required to observe each source. The Arecibo telescope slew times are $0\overset{\circ}{.}4\ {\rm s}^{-1}$ in azimuth and $0\overset{\circ}{.}04\ {\rm s}^{-1}$ in elevation. A 1° change in elevation will require 25 s. It will thus be observationally advantageous if the sky density of tentative sources to be corroborated is high, e.g., on the order of 1 $\deg^{-2}$ or higher. Not only will that reduce the overhead of slew motions and settle time, but it will also allow for a running mean bandpass to be accumulated over a few contiguous staring observations, as the telescope configuration would change little between adjacent source candidates. In that case, allowing for slew and settle time, a corroborating observation of a single source will require on the order of 1–2 minutes of telescope time. The steeply rising fraction of false sources with decreasing s suggests that corroborating observations requesting single-pixel telescope time at the level of approximately 10% of the request proposed for the ALFA observations will deliver optimal returns.

8. SUMMARY

ALFALFA uses the new seven-beam Arecibo L-band Feed Array (ALFA) to carry out a wide-area survey of the high Galactic latitude sky visible from Arecibo. In addition to the all-important sensitivity advantage that accrues from using Arecibo, the world's most sensitive radio telescope at the L band, ALFA offers important and significant improvements in angular and spectral resolution over the available major wide-area extragalactic H I line surveys, such as HIPASS and HIJASS. ALFALFA is intended to produce an extensive database of H I spectra that will be of use to a broad community of investigators, including many interested in the correlative mining of multiwavelength data sets. It is specifically designed to probe the faint end of the HIMF in the very local universe.

As a result of practical considerations and simulations of survey efficiency, ALFALFA exploits a simple fixed-azimuth drift-scanning technique: minimum intrusion. A two-pass strategy will greatly aid in the rejection of spurious signals and RFI, thus minimizing the need for follow-up confirmation observations, evening out the scalloping in the maps that arises from unequal pixel gain, and offering the opportunity to use the same data set for the statistical characterization of continuum transients. Initial tests of the hardware, software, and survey observing mode, conducted in fall 2004 during the ALFA commissioning phase as described in Paper II, confirm the efficacy of the planned approach. The basic parameters of the ALFALFA survey can be summarized accordingly as follows:

1. Sky coverage is 7074 $\deg^2$, between 0° and $+36^\circ$ in declination, $07^{\rm h}30^{\rm m}$–$16^{\rm h}30^{\rm m}$ and $22^{\rm h}00^{\rm m}$–$03^{\rm h}00^{\rm m}$ in right ascension, with $3\overset{\prime}{.}5$ spatial resolution.
2. Frequency coverage is between 1335 and 1435 MHz, yielding coverage of extragalactic H I in redshift out to $cz < 18{,}000\ {\rm km\ s^{-1}}$, with 5.3 $\rm km\ s^{-1}$ maximum spectral resolution.
3. Sensitivity is $1.8({\rm res}/10)^{-1/2}$ mJy per beam area, where res is the spectral resolution in kilometers per second.
4. On the order of 20,000 H I sources are expected to be detected by the survey. Extragalactic H I sources with $M_{\rm H\,I} \simeq 10^6\ M_\odot$ will be detectable to a distance of 6.5 Mpc, while H I masses $M_{\rm H\,I} \simeq 10^7\ M_\odot$ will be detectable throughout most of the Local Supercluster, including the Virgo Cluster and out to 20 Mpc. Several hundred sources will have $M_{\rm H\,I} < 10^{7.5}\ M_\odot$, thus allowing a robust determination of the faint end of the HIMF.
5. Public-access data products will be produced on a continuing basis as subsets (tiles) of the overall survey are completed.

Observations for ALFALFA started in 2005 February, and completion of the survey is expected to take 5–6 yr. Cataloging a complete census of H I locally, pinning down the HIMF to the lowest masses, and conducting the blind H I absorption and OH megamaser surveys will require completion of the full 5 yr program, but even the initial 2005 allocation promises early science results in several important areas. These areas include the mapping of nearly 1600 $\deg^2$, more than 3 times the coverage with twice the sensitivity of the Arecibo Dual Beam Survey (Rosenberg & Schneider 2000); a first blind census across the Virgo Cluster region with a detection limit of $M_{\rm H\,I} > 10^7\ M_\odot$ at the cluster distance (assuming a width $W = 30\ {\rm km\ s^{-1}}$); a complete search for HVCs around M33; the identification of gas-rich galaxies in the NGC 784 and Leo I groups; the mapping of the environments of 12 gas-rich galaxies with $D_{\rm UGC} > 7'$; and a first attempt at a large blind survey for H I absorbers.

R. G. and M. P. H. acknowledge the partial support of NAIC as Visiting Scientists during the period of this work. This work has been supported by NSF grants AST 03-07661, AST 04-35697, AST 03-47929, AST 04-07011, and AST 03-02049; DGICT of Spain grant AYA2003-07468-C03-01; and a Brinson Foundation grant. We thank the director of NAIC, Robert Brown, for stimulating the development of major ALFA surveys; Enzo Branchini for providing a PSCz density grid in digital form; Héctor Hernández for a sensible and friendly approach to telescope scheduling; and the director, telescope operators, and support staff of the Arecibo Observatory for their proactive assistance.

REFERENCES

Barnes, D. G., et al. 2001, MNRAS, 322, 486
Begum, A., Chengalur, J. N., & Karachentsev, I. D. 2005, A&A, 433, L1
Branchini, E., et al. 1999, MNRAS, 308, 1
Broeils, A., & Rhee, M.-H. 1997, A&A, 324, 877
Corbelli, E., & Bandiera, R. 2002, ApJ, 567, 712
Cortés-Medellín, G. 2002, NAIC Internal Memo 02-08
Darling, J., & Giovanelli, R. 2002, ApJ, 572, 810
Davies, J., et al. 2004, MNRAS, 349, 922
de Vaucouleurs, G., de Vaucouleurs, A., Corwin, H. G., Buta, R. J., Paturel, G., & Fouqué, P. 1991, Third Reference Catalogue of Bright Galaxies (New York: Springer)
Giovanelli, R., & Brown, R. L. 1973, ApJ, 182, 755
Giovanelli, R., et al. 2005, AJ, 130, 2613 (Paper II)
Haynes, M., Giovanelli, R., & Roberts, M. S. 1979, ApJ, 229, 83
Hewitt, J. N., Haynes, M. P., & Giovanelli, R. 1983, AJ, 88, 272
Hoffman, G. L., Lu, N. Y., & Salpeter, E. E. 1992, AJ, 104, 2086
Karachentsev, I. D., Karachentseva, V. E., Huchtmeier, W. K., & Makarov, D. 2004, AJ, 127, 2031
Kerr, F. J., & Hindman, J. V. 1953, AJ, 58, 218
Kildal, P. S., Johansson, M., Hagfors, T., & Giovanelli, R. 1993, IEEE Trans. Antennas Propag., 41, 1019
Krumm, N., & Burstein, D. 1984, AJ, 89, 1319
Lang, R. H., et al. 2003, MNRAS, 342, 738
Masters, K. L., Haynes, M. P., & Giovanelli, R. 2004, ApJ, 607, L115
Meyer, M. J., et al. 2004, MNRAS, 350, 1195
Minchin, R. F., et al. 2005, ApJ, 622, L21

Oosterloo, T., & van Gorkom, J. 2005, A&A, 437, L19
Roberts, M. S. 1975, in Galaxies and the Universe, ed. A. Sandage, M. Sandage, & J. Kristian (Chicago: Univ. Chicago Press), 309
Rosenberg, J. L., & Schneider, S. E. 2000, ApJS, 130, 177
———. 2002, ApJ, 567, 247 (RS02)
Schneider, S. E., Helou, G., Salpeter, E. E., & Terzian, Y. 1983, ApJ, 273, L1
Springob, C. M., Haynes, M. P., & Giovanelli, R. 2005a, ApJ, 621, 215
Springob, C. M., Haynes, M. P., Giovanelli, R., & Kent, B. R. 2005b, ApJS, 160, 149
Swaters, R. A., van Albada, T. S., van der Hulst, J. M., & Sancisi, R. 2002, A&A, 390, 829
Thilker, D., Braun, R., Walterbos, R. A. M., Corbelli, E., Lockman, F. J., Murphy, E., & Maddalena, R. 2004, ApJ, 601, L39
van Zee, L. 2005, ApJ, submitted
Westmeier, T., Braun, R., & Thilker, D. 2005, A&A, 436, 101
Zwaan, M. A., Briggs, F. H., Sprayberry, D., & Sorar, E. 1997, ApJ, 490, 173 (Z97)
Zwaan, M. A., Meyer, M. J., Staveley-Smith, L., & Webster, R. L. 2005, MNRAS, 359, L30 (Z05)
Zwaan, M. A., et al. 2004, MNRAS, 350, 1210 (Z04)